Journal of Aerosol Science 191 (2026) 106709



Contents lists available at ScienceDirect

Journal of Aerosol Science

journal homepage: www.elsevier.com/locate/jaerosci





A new aerosol respiratory deposition approach: Health risks of metals in aerosols from electronic nicotine delivery systems and heated tobacco products

Jinho Lee *, Wei-Chung Su

Department of Environmental and Occupational Health Sciences, School of Public Health, University of Texas Health Science Center at Houston, TX, 77030, USA

ARTICLE INFO

Keywords:
Respiratory deposition
Deposited mass
E-cigarette aerosol
Heated tobacco aerosol
Health risk

ABSTRACT

This study employed a newly developed MALDA-MOUDI approach to investigate the respiratory deposition of Electronic Nicotine Delivery Systems (ENDS) and Heated Tobacco Products (HTP) aerosol and used the resulting data to assess associated health risks. MALDA-MOUDI is a tandem system that integrates the Mobile Aerosol Lung Deposition Apparatus (MALDA) with the Micro-Orifice Uniform Deposit Impactor (MOUDI) to enable effective estimations of the size-dependent deposited mass of inhaled aerosol in major airway regions. The MALDA-MOUDI system covers a wide particle size range, from nanometers to micrometers, making it ideal for comprehensive aerosol exposure research. To study ENDS and HTP aerosol respiratory deposition using MALDA-MOUDI, a series of laboratory experiments was conducted to obtain the deposited mass of ENDS and HTP aerosol in human airways. Two types of ENDS and one HTP (JUUL, disposable, and IQOS) were used in the study to generate test aerosol. MALDA-MOUDI respiratory deposition experiments were carried out under both active (mainstream) and passive (secondhand) exposure conditions. Metal-induced health risks were systematically evaluated based on the measured respiratory deposited mass under presumed active and passive use scenarios. The acquired results indicated that non-cancer and cancer risks associated with metals released from the tested ENDS and HTP fell within acceptable levels for both active and passive use scenarios. The MALDA-MOUDI system is a valuable tool for aerosol respiratory deposition studies and can be applied to broader environmental and occupational aerosol exposure research to assess health risks associated with toxic substances in aerosol particles.

1. Introduction

The study of aerosol respiratory deposition is an indispensable component of aerosol research. Inhalation of aerosol can result in a portion of inhaled particles depositing in the respiratory tract, with deposition fractions varying by particle size (International Commission on Radiological Protection, 1994; Miller et al., 2016; National Committee on Radiation Protection and Measurements, 1997). The deposited particles can introduce toxic substances into the airways, leading to potential lung problems, such as chronic

This article is part of a special issue entitled: Inhaled Aerosol Dosimetry published in Journal of Aerosol Science.

* Corresponding author. Department of Environmental Health, School of Public Health, Boston University, Talbot W Building, 715 Albany Street, Boston, MA, 02118, USA.

E-mail address: jinholee@bu.edu (J. Lee).

https://doi.org/10.1016/j.jaerosci.2025.106709
Received 24 April 2025; Received in revised form 1 September 2025; Accepted 23 October 2025
Available online 30 October 2025
0021-8502/© 2025 Elsevier Ltd. All rights are reserved, including those for text and data mining, AI training, and similar technologies.

bronchitis, asthma exacerbation, and reductions in pulmonary function, and other health effects (Hinds & Zhu, 2022). Therefore, understanding aerosol respiratory deposition following aerosol exposure is crucial, particularly from a public health perspective. However, conducting aerosol respiratory deposition experiments was challenging in the past due to the need for specialized facilities, instruments, and protocols (Cheng et al., 1993; Cohen et al., 1990). Moreover, most published aerosol respiratory deposition experiments have focused on the human upper airways, as fabricating lower airway replicas was difficult (Kelly et al., 2004; Zhou & Cheng, 2005). Consequently, the applicability of previously acquired respiratory deposition data in etiological research was limited because the deeper regions of the respiratory tract are the primary sites of many adverse lung effects from aerosol exposure (Brown et al., 2002; Oberdörster et al., 2005). The experimental data on aerosol deposition in the human lower airways remain scarce.

To address the limitations of prior aerosol respiratory deposition experiments, the Mobile Aerosol Lung Deposition Apparatus (MALDA) was developed. MALDA comprises a set of 3D-printed human airway replicas, and was designed based on the anatomy of human respiratory tracts and a theoretical model (Su et al., 2019, 2021). These airway replicas encompass the human upper airways, including the nasal and oral passages, throat, and trachea, as well as the lower airways, with the tracheobronchial (TB) airways down to the 11th lung generation and a representative alveolar region, fabricated by filling a conductive PLA casing with conductive porous foam. The details about the structure of the MALDA are represented in our previous publications (Lee & Su, 2025; Su et al., 2019, 2021).

By using a pair of particle sizers to measure the variations in the particle size distributions of the inhaled aerosol particles across major airway regions (head airway, TB tree, and alveolar region), size-dependent aerosol respiratory deposition fractions in the human airways can be systematically estimated (Su et al., 2023, 2024). It's worth noting that the initial version of MALDA was designed to target particles in the nanometer (ultrafine) size range; therefore, it can be referred to as Nano-MALDA. Recently, another MALDA set tailored for micrometer-sized aerosol (Micro-MALDA) was successfully developed (Lee & Su, 2025). By operating Micro-MALDA in conjunction with Nano-MALDA, the applicable aerosol size range of the MALDA system was significantly expanded from the nanometer to the micrometer scale. These two MALDA sets enable a comprehensive measurement of aerosol respiratory deposition, covering particle sizes commonly encountered in real-world aerosol exposure scenarios. To further enhance the capability of MALDA, the MALDA sets were connected (individually) to a commercially available size-segregated aerosol sampler - Micro-orifice Uniform Deposit Impactor (MOUDI, model 110-R, MSP Co., Shoreview, MN, USA). This integration resulted in a MALDA-MOUDI tandem system, allowing a more effective and detailed analysis of the deposited mass of inhaled aerosol in major airway regions across a broad particle size range (Lee & Su, 2025).

Over the past few decades, the global use of Electronic Nicotine Delivery Systems (ENDS) and Heated Tobacco Products (HTP) has grown rapidly, particularly among younger populations (Ali et al., 2020; McKelvey et al., 2018). One of the factors driving the surge is the common perception that ENDS and HTP are a safer alternative to traditional tobacco cigarettes. It is widely recognized that adverse health effects from cigarette smoking are primarily linked to tobacco combustion. Thus, ENDS and HTP use, which does not involve tobacco combustion, has gained popularity, particularly among teenagers and young adults (Buu et al., 2020; Cullen et al., 2018; McKelvey et al., 2018). Although evidence suggests that using ENDS or HTP produces overall lower aerosol concentrations compared to cigarette smoking (McAuley et al., 2012; Pacitto et al., 2018; Papaefstathiou et al., 2020), frequent use of them can degrade indoor air quality and result in secondhand exposure to ENDS or HTP aerosol constituents, such as ultrafine particles and nicotine (Bekki et al., 2017; Logue et al., 2017; Protano et al., 2017). Research has also reported that ENDS and HTP aerosols contain organic compounds (e.g., 2,3-pentanedione, diacetyl) and metals (e.g., Cr, Pb, Mn, Zn) (Allen et al., 2016; Amorós-Pérez et al., 2022; Olmedo et al., 2018; Uchiyama et al., 2015). Several investigations imply that inhalation of these constituents can trigger oxidative stress and inflammation, and impair lung function in animals and humans (Areecheewakul et al., 2020; Hubbs et al., 2008, 2012; Staudt et al., 2018). Given the rising prevalence of ENDS and HTP use and the fact that comprehensive regulations are still absent in many countries worldwide—for example, the United Kingdom bans indoor combustible-cigarette smoking but sets no product-specific limits on ENDS (Public Health England, 2016)—both active and passive exposure to them have emerged as significant public-health concerns, potentially fostering nicotine dependence among non-smokers, and complicating efforts to curb combustible-cigarette use. (National Academies of Sciences, Engineering, and Medicine, 2018; Soneji et al., 2017). Therefore, accurately assessing the health risks of active and passive exposure to ENDS and HTP is essential, and such evaluations must be grounded in the thorough investigation of aerosol respiratory deposition.

With this in mind, the purpose of this study was to apply the newly developed MALDA-MOUDI system to assess potential health risks associated with toxic metals in ENDS and HTP aerosol. Evidence indicates that ENDS and HTP aerosols contain various potentially harmful metals (Bekki et al., 2017; Gray et al., 2022; Olmedo et al., 2018), and such metals deposited in the human airways may contribute to a variety of lung conditions, including lung inflammation, decreased lung function, and even lung cancer (Areecheewakul et al., 2020; Bracken-Clarke et al., 2021; Monsé et al., 2021; Shehata et al., 2023). In this study, to examine the health impact of ENDS and HTP aerosol exposure, a series of laboratory-based aerosol respiratory deposition experiments were conducted using the MALDA-MOUDI approach under both active and passive exposure conditions. The deposited mass of metals in the respiratory tract was carefully estimated and subsequently used to assess potential health risks.

2. Methods

2.1. MALDA-MOUDI tandem system

The MALDA-MOUDI system has been demonstrated to generate reliable, size-dependent respiratory aerosol deposition data that closely match conventional lung deposition curves, making it well-suited for aerosol exposure studies (Lee & Su, 2025). Fig. 1

illustrates the MALDA-MOUDI system and the experimental procedure to determine the deposited mass of inhaled aerosol in major airway regions. During the MALDA-MOUDI experiments, Micro-MALDA and Nano-MALDA were individually connected to the MOUDI. Since Nano-MALDA, Micro-MALDA, and MOUDI all operate at the same flow rate (30 L/min), they can be used simultaneously in an integrated configuration. Based on the experimental design, the size-dependent (d-dependent) deposited mass of aerosol in a specific airway region ($DM_{airway,d}$) can be obtained by:

$$DM_{Head+TB,d} = M_{o,d} - M_{Head+TB,d}, \tag{1}$$

$$DM_{Alv,d=}M_{Head+TB,d} - M_{Head+TB+Alv,d}, \tag{2}$$

$$DM_{Total,d} = DM_{Head+TB,d} + DM_{Alv,d}, \tag{3}$$

where, $M_{o,d}$ is the size-dependent mass concentration of test aerosol collected by MOUDI when no airway replicas are connected to the inlet of MOUDI. $M_{Head+TB,d}$, is the size-dependent mass concentration obtained by MOUDI when the head airways and TB airways are connected at the inlet of MOUDI. $M_{Head+TB+Alv,d}$ is the size-dependent mass concentration obtained by MOUDI when the entire airway replica set (from the head airways to the alveolar region) is connected to MOUDI. The size-dependent mass concentration of the test aerosol was determined by weighing the filters retrieved from MOUDI using a microbalance (CAHN-35, ThermoFisher, Waltham, MA, USA). According to the design of MOUDI, filters are positioned across eleven impaction stages, with each stage (filter) capturing aerosol samples within distinct aerodynamic diameter ranges. $DM_{Head+TB,d}$, $DM_{Alv,d}$, and $DM_{Total,d}$ represent the size-dependent deposited mass of the test aerosol in the head-to-TB airways, the alveolar region, and the entire human respiratory tract, respectively.

2.2. Products and aerosol generation

Three products were used in this study for both active and passive exposure experiments. The selected products include a disposable e-cigarette (Onee Stick, Kangvape Technology, Shenzhen, China), a single-use vape pod e-cigarette (JUUL, JUUL Labs, Washington D.C., USA), and an HTP device (IQOS ILUMA, Philip Morris, Stamford, CT, USA). All products were purchased from licensed US retailers no more than 1 month before testing, and stored unopened at room temperature (15–25 °C), low humidity, and out of direct light. The purchased disposable e-cigarettes, JUUL cartridges, and IQOS sticks were opened immediately before use and tested the same day.

These three non-combustible nicotine products were selected to represent various recent technologies, including the most popular types of ENDS—disposable devices, single-use pod systems—as well as HTP, which are expected to grow in market share. To generate ENDS and HTP aerosol for respiratory deposition experiments, a puffing machine (CSM-eSTEP, CH Technologies, Inc., Westwood, NJ) was employed. The puffing topography (frequency, volume, duration, volume, etc.) was set to 2 puffs per minute, with each puff having a volume of 55 ml and a duration of 3 s. These parameters align with those specified by the International Organization for

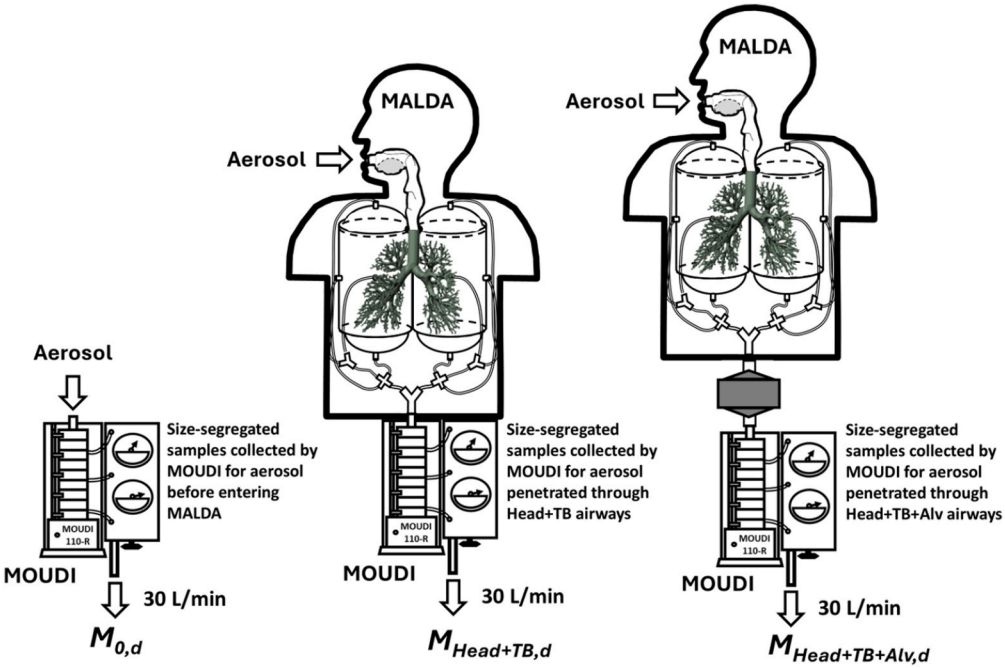


Fig. 1. MALDA-MOUDI system and the procedure to obtain the deposited mass of inhaled aerosol in different airway regions using Eqs. (1)–(3).

Standardization (ISO) 20768. We employed this method since it is the current inter-laboratory standard and lies within the range of puff volumes for users (International Organization for Standardization, 2018).

2.3. Aerosol respiratory deposition experiments

For respiratory deposition experiments under active exposure conditions, the ENDS and HTP aerosol generated by the puffing machine was delivered directly to the MALDA-MOUDI tandem system (Fig. 2(a)). In the passive exposure experiments, the ENDS and HTP aerosols were first routed through a temperature (T) and relative humidity (%RH) conditioner to simulate the conditions the aerosol encounters within an active user's lung before being exhaled. The T and %RH conditioner was maintained at 37 °C and ~100 % RH (Déry et al., 1967; Man et al., 1979). The conditioned aerosol was then transported to the stainless-steel dilution chamber before being delivered to the MALDA-MOUDI system (Fig. 2(b)). The main compartment of the dilution chamber measured 61 cm (L) × 61 cm (W) × 61 cm (H). The chamber was equipped with an electronic fan, and we assumed that the aerosols were well-mixed inside the chamber. Temperature and relative humidity in the chamber were maintained at 20–25 °C and 50 ± 10 % RH, respectively, replicating standard indoor thermal environmental conditions (American Society of Heating, Refrigerating and Air-Conditioning Engineers, 2023).

During the respiratory deposition experiment, 10 to 20 puffs of ENDS and HTP aerosol were generated. This puff range was optimized through a set of preliminary trials to ensure adequate aerosol mass collection on MOUDI filters, allowing sufficient aerosol samples to load on filters for small particles while preventing overload on filters for large particles. The filter installed in MOUDI for

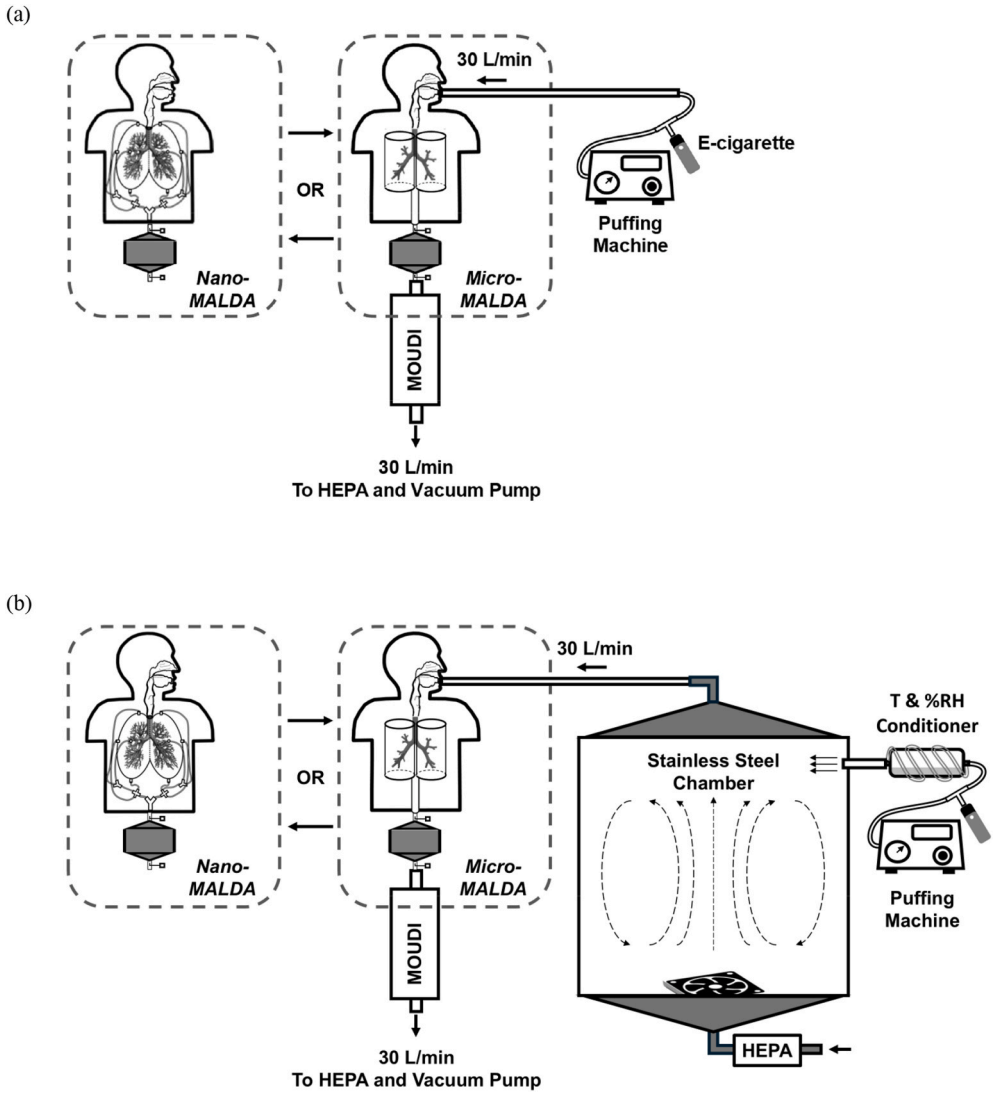


Fig. 2. The schematic of the experimental setup for (a) active vaping, and (b) passive vaping using the MALDA-MOUDI tandem system.

aerosol collection was a 37 mm Polytetrafluoroethylene (PTFE) membrane filter (R2PJ037, PALL Co., Port Washington, NY, USA). After the experiment, PTFE filters were immediately removed from the MOUDI and weighed using a microbalance to minimize mass loss from solvent evaporation. Filters were then placed in separate Petri dishes and stored in a freezer for subsequent metal analysis.

MOUDI was cleaned with isopropanol alcohol (IPA) after each experiment to prevent cross-contamination. The human airway replicas in both Nano-MALDA and Micro-MALDA were also flushed with IPA after every five experimental runs. Following the airway cleaning, the inner surfaces of the airway replicas were recoated with a thin layer of fresh silicone oil (S159-500, Fisher Scientific International, Inc., Pittsburgh, USA) to maintain consistent surface properties. The airway systems of Micro-MALDA and Nano-MALDA were periodically re-evaluated to ensure their performance.

To verify that the ENDS and HTP aerosol respiratory deposition data obtained from the MALDA-MOUDI approach is comparable to conventional lung deposition curves (International Commission on Radiological Protection, 1994), the regional deposited mass of aerosol was used to calculate deposition fractions in the corresponding airway regions using the following equations:

$$DF_{Head+TB,d} = DM_{Head+TB,d} / M_{o,d} \tag{4}$$

$$DF_{Alv,d} = DM_{Alv,d} / M_{o,d} \tag{5}$$

$$DF_{Total,d} = DM_{Total,d} / M_{o,d} \tag{6}$$

where $DM_{Head+TB,d}$, $DM_{Alv,d}$, $DM_{Total,d}$ and $M_{o,d}$ have been defined previously. $DF_{Head+TB,d}$ $DF_{Alv,d}$ and $DF_{Total,d}$ are the size-dependent aerosol respiratory deposition fractions (ranging from 0 to 1) in the head-to-TB airways, the alveolar region, and the entire human respiratory tract, respectively. To further compare the aerosol respiratory deposition fractions obtained from the MALDA-MOUDI approach with those from the previously adopted method using MALDA alone, additional aerosol respiratory deposition experiments (particle number-based) were conducted using only the two MALDA sets (without MOUDI). In the particle number-based experimental approach, respiratory deposition fractions were determined by particle sizers. The Scanning Mobility Particle Sizer (SMPS, NanoScan 3910, TSI Inc., Shoreview, MN, USA) was used for nanometer-sized particles, while the Aerodynamic Particle Sizer (APS, Model 3321, TSI Inc., Shoreview, MN, USA) was employed for micrometer-sized particles. Given that a total flow of 30 L/min was required to operate the two MALDA sets, the sampling probes for real-time monitoring devices were designed with stainless steel tubing of suitable diameter to match the MALDA flow rate and connected to the SMPS and APS.

The major physical properties (e.g., particle diameter) of ENDS and HTP aerosols can shift markedly with both the dilution ratio and the residence time of the sampled plume. Consequently, comparable size-distribution measurements demand consistent dilution and residence time (David et al., 2020; Kane & Li, 2021; Lalo et al., 2020; Luo et al., 2021). Under these operating conditions, our passive exposure experimental settings represented an air-change rate of 8.33 h^{-1} and an overall dilution ratio of approximately 270:1. To prevent impactor over-loading and to ensure reliable SMPS/APS readings, we empirically set a maximum aerosol concentration, which was <1 % of the particle-number concentration at which coincidence-counting artefacts have been reported (Oldham et al., 2023) (see Section 3.1 for details). This threshold was applied to both passive and active exposure experiments to avoid potential measurement errors. For both mass-based and number-based studies, each experimental condition was repeated three times to obtain statistically meaningful averages and standard deviations.

2.4. Aerosol metal composition analysis

To analyze the metal constituents in size-segregated aerosol by ICP-MS, MOUDI filters with collected aerosol were prepared according to the EPA IO-3 method (U.S. EPA, 1999). Metal analysis was performed at an ISO 17025-accredited commercial laboratory in Houston, USA. A total of 20 metals (Al, Sb, As, Be, Cd, Cr, Co, Cu, Fe, Pb, Mn, Mo, Ni, Se, Ag, Sr, Sn, Ti, V, and Zn) were targeted based on published research (Gray et al., 2019, 2022; Hess et al., 2017; Olmedo et al., 2018). For each set of MOUDI filters, a blank filter was provided and analyzed alongside the sample filters to determine the background metal concentration. The metal concentration in each sample was calculated by subtracting the metal concentration of the blank filter (blank-adjusted metal concentration). If the blank-adjusted metal concentration of a target metal was below the limit of detection (LOD) of the instrument, the concentration of that metal was recorded as non-detect (N.D.).

2.5. Deposited dose estimation

Once the size-dependent respiratory deposited mass data were acquired from the MALDA-MOUDI experiments and the size-dependent metal constituent data were available from the ICP-MS metal analysis, the deposited dose of a target metal in the bodies of actively and passively exposed individuals could be estimated. For active exposure studies, the per-puff, size-dependent respiratory deposited dose of a target metal k ($PDD_{k,d}$, ng/kg-puff) in an active user's body was calculated using the following equation:

$$PDD_{k,d} = \left(DM_{Total,d} \times C_{k,d} \times IR\right) / \left(BW \times Q \times N\right) \tag{7}$$

where $DM_{Total,d}$ was calculated using Eq. (3). $C_{k,d}$ represents the size-dependent mass fraction (ranging from 0 to 1) of the target metal k in ENDS and HTP aerosol. $C_{k,d}$ was determined by the ratio of the mass of the target metal obtained from a filter to the mass of aerosol collected on the same filter. IR is the human inhalation rate per hour, set at 15 L/min. BW is the average human body weight, which is

70 kg (U.S. EPA, 2011). Q refers to the flow rate used in the MALDA-MOUDI experiment (30 L/min). N denotes the number of puffs generated during each active exposure experiment.

For passive exposure studies, the hourly size-dependent respiratory deposited dose of a target metal k ($HDD_{k,d}$, ng/kg-hr) was estimated using the following equation:

$$HDD_{k,d} = \left(DM_{Total,d} \times C_{k,d} \times IR\right) \ / \ (BW \times Q \times T) \tag{8}$$

where the definition of $DM_{Total,d}$, $C_{k,d}$, IR, and BW remain the same as previously described. The inspiratory flow rate Q of 30 L/min corresponds to the minute ventilation rate of an adult during light activities (NCRP, 1997). T represents the experimental time (in hours) used in each passive exposure experiment.

The estimated $PDD_{k,d}$ and $HDD_{k,d}$ were then summed across the particle size (d) to calculate the size-cumulative per-puff deposited dose (PDD_k) for active exposure, and the size-cumulative hourly deposited dose (HDD_k) for passive exposure.

2.6. Health risk assessment

With the PDD_k and HDD_k calculated, the average daily dose (ADD_k, ng/kg-day) and the lifetime average daily dose ($LADD_k$, ng/kg-day) of a metal could be reasonably estimated for both active and passive exposure scenarios. For active exposure, the average daily dose (A_ADD_k) and the lifetime average daily dose (A_LADD_k) of the target metal k were determined using the following equations:

$$A_ADD_k = \frac{PDD_k \times CR \times CT}{AT} \tag{9}$$

$$A_LADD_k = \frac{PDD_k \times CR \times CT}{LE} \tag{10}$$

where the contact rate (CR) of active users to ENDS and HTP aerosol was set at 365 puffs/day, based on previously published studies on the average puff frequency among exclusive e-cigarette users (Aherrera et al., 2020). We considered this value appropriate as a health-protective worst-case assumption, since the recent studies reported that the upper-percentile consumption of pod-type devices, such as JUUL, was about 300 puffs/day (Tillery et al., 2023), and established IQOS users were also assumed to use at least 300 puffs/day (Cheng et al., 2025). CT represents the contact time (years) of active users. AT denotes the averaging time (years) used to estimate ADD_k for active use of ENDS and HTP. In this study, both CT and AT were assumed to be 36.4 years, according to published data (Bhatt et al., 2018). The lifetime expectancy (LE) was considered to be 70 years (U.S. EPA, 2011).

For passive exposure, the average daily dose (P_ADD_k) and the lifetime average daily dose (P_LADD_k) of the target metal k were estimated using a similar approach:

$$P_ADD_k = \frac{HDD_k \times CR \times CT}{AT} \tag{11}$$

$$P_LADD_k = \frac{HDD_k \times CR \times CT}{LE} \tag{12}$$

where CT, AT, and LE are the same values as described for active use. The contact rate (CR) in passive exposure, which is an average daily exposure duration for a passively exposed individual to secondhand ENDS and HTP aerosol was assumed as 4 h/day. This figure is grounded in a worst-case scenario in which a non-user remains with the user in the same shared indoor space that is not subject to vaping/using prohibitions (e.g., a private home). With 365 puffs per day at 30 s per puff, the total use time comes to roughly 3.0 h; we rounded this figure up to 4 h to include a health-protective buffer, to account for the lingering aerosol in the room air after active users' vaping/using sessions, as it takes time for the aerosol's natural dissipation.

The calculated average daily dose, A_ADD_k and P_ADD_k, were then utilized to estimate the non-cancer health risks using the hazard quotient (HQ_k), which was determined through dividing A_ADD_k and P_ADD_k by the published reference dose of the target metal k (RfD_k). To account for the additive health effects from different metals, the hazard index (HI) was calculated by the summation of relevant HQ_k values. On the other hand, the calculated lifetime average daily dose, A_LADD_k and P_LADD_k, were multiplied by the published cancer slope factor of the target metal k (CSF_k) to assess the excess lifetime cancer risk associated with the target metal found in ENDS and HTP aerosol. The published RfD_k and CSF_k values (or their conversion equivalents) used in this study to assess non-cancer and cancer risks for a target metal k were sourced from publicly available databases or websites, including the EPA Integrated Risk Information System (IRIS), the California EPA Office of Environmental Health Hazard Assessment (OEHHA), and the (Agency for Toxic Substances and Disease Registry, 2024; California Environmental Protection Agency, 2024; U.S. EPA, 2024). For both active and passive exposure, the estimated non-cancer risk is deemed unacceptable if the calculated HQ_k or HI exceeds 1.0, suggesting a potential non-cancer effect. The cancer risk is considered unacceptable if the calculated excess lifetime cancer risk for the target metal k exceeds 1.0×10^{-6}.

3. Results

3.1. Aerosol respiratory deposition

Fig. 3 illustrates the particle size distribution of aerosol generated by the three test products. As shown in Fig. 3(a), for number-based particle size distribution, the disposable e-cigarette and JUUL exhibited a bimodal size distribution under active and passive exposure conditions, whereas the IQOS produced a unimodal distribution in both exposure conditions. Notably, a substantial fraction of the aerosol generated from the tested products fell within the nanoparticle size range. In Fig. 3(b), the mass-based particle size distributions showed a bimodal pattern under active exposure for all test products, but showed a unimodal distribution under passive exposure. Overall, active exposure represented higher aerosol mass concentrations than passive exposure. The mass median diameters (MMADs) measured 0.57 μm (disposable), 0.58 μm (JUUL), and 0.21 μm (IQOS) during active exposure, with corresponding values of 0.51 μm, 0.59 μm, and 0.31 μm during passive exposure.

Figs. 4 and 5 show the aerosol size-dependent respiratory deposition fractions obtained from the mass-based MALDA-MOUDI

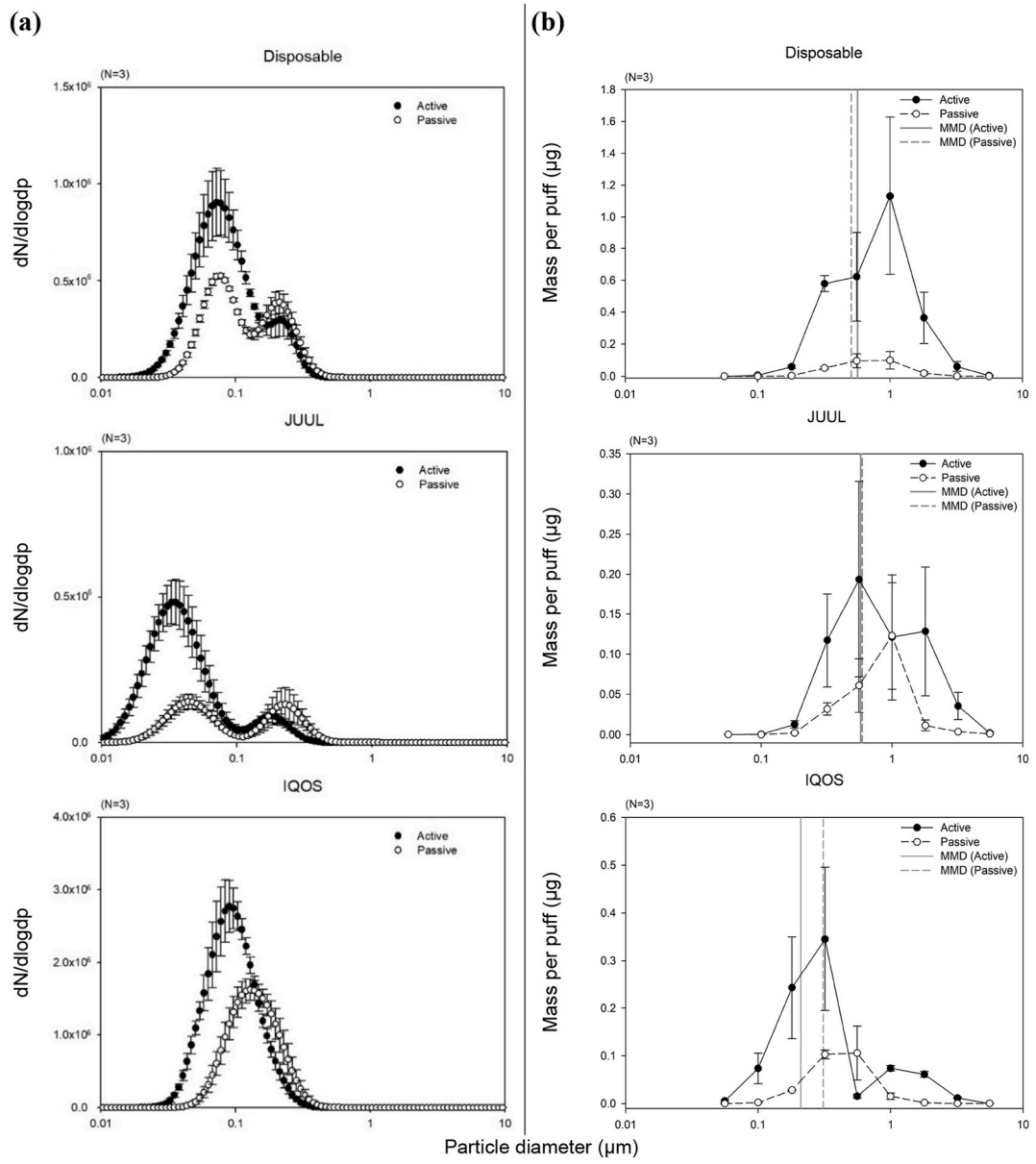


Fig. 3. Average size distribution of e-cigarette aerosol: (a) number-based size distribution, and (b) mass-based size distribution (error bars indicating the standard deviation).

approach via Eqs. (1)–(6), and from the number-based method using MALDA alone. Also shown in the figures are the corresponding ICRP lung deposition curves. The mass-based and number-based data exhibited general consistency in their trends across the nanometer to micrometer size range. Additionally, Figs. 4 and 5 express a general similarity in deposition patterns and values, regardless of the ENDS or HTP products, or their use conditions. This similarity may be attributed to the liquid-based nature of ENDS and HTP aerosol and the predominantly spherical morphology of them, as commonly assumed (National Academies of Sciences, Engineering, and Medicine, 2018).

Fig. 6 displays the respiratory deposited mass in the head-to-TB airways, alveolar region, and the entire human airways (total) obtained by the MALDA-MOUDI tandem system for the three test products under active and passive exposure conditions. It can be seen that the particle sizes associated with significant respiratory deposited mass closely correspond to the mode size of the mass-based size distributions shown in Fig. 3.

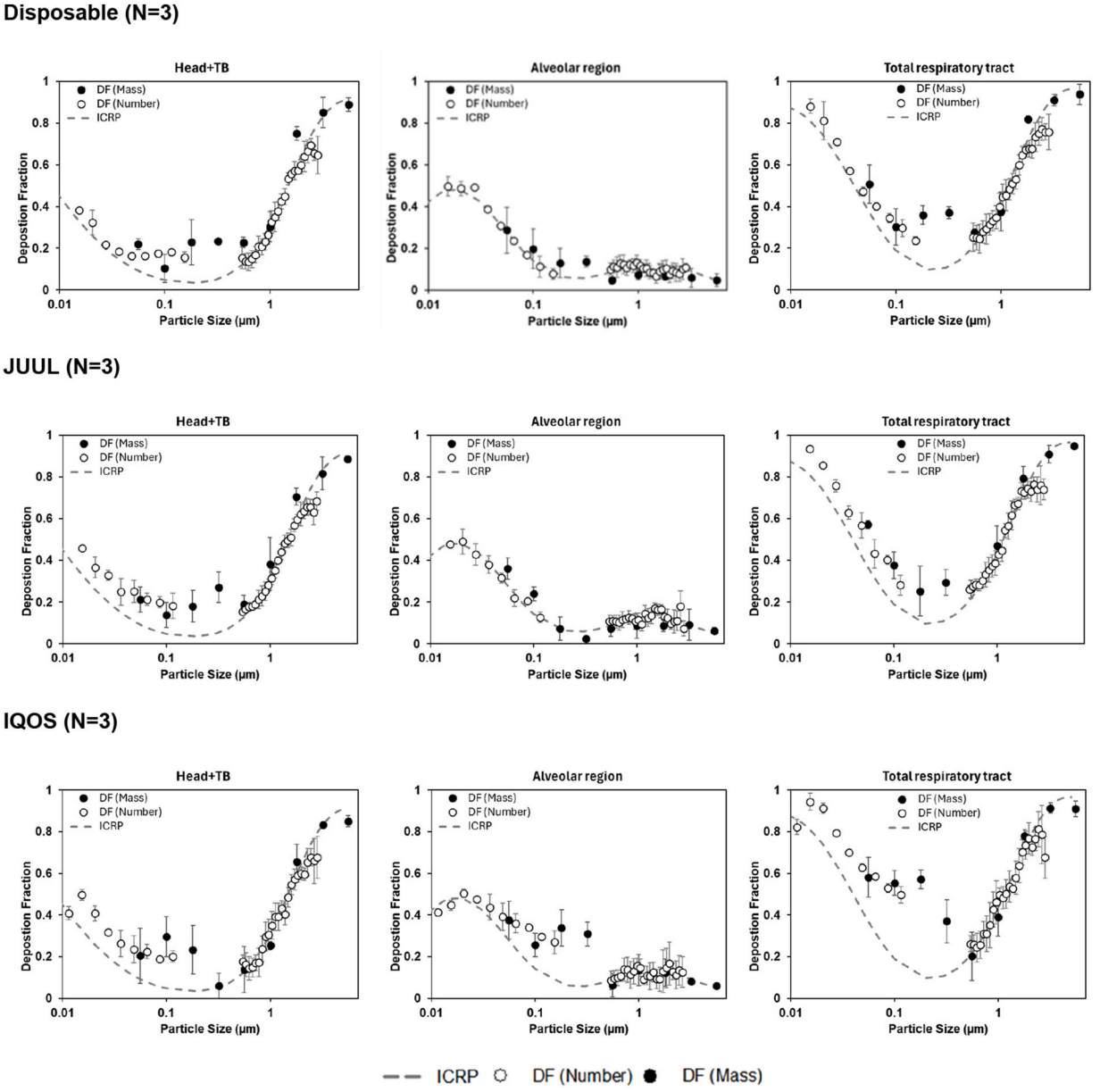


Fig. 4. E-cigarette aerosol respiratory deposition fractions for active vaping (error bars indicating the standard deviation).

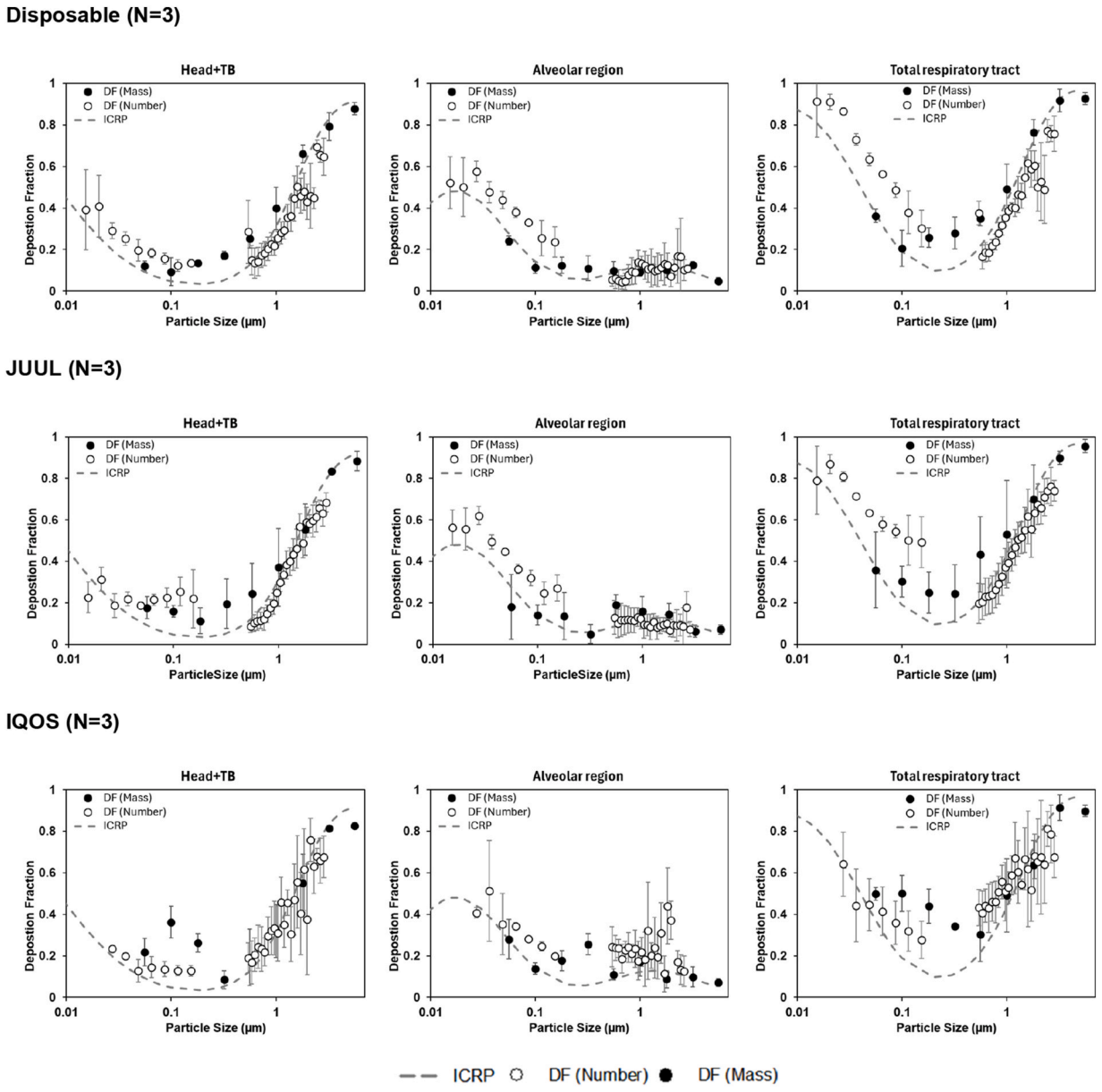


Fig. 5. E-cigarette aerosol respiratory deposition fractions for passive vaping (error bars indicating the standard deviation).

3.2. Aerosol metal constituent

The ICP-MS metal analysis revealed that seven out of the twenty target metals (Cr, Cu, Al, Zn, Ti, Pb, and V) were detected at quantities exceeding the LOD. The total mass of these detected metals on each MOUDI filter was summed and compared to the corresponding aerosol mass collected on the same filter. Fig. 7 presents the average size-dependent metal-to-aerosol mass ratio for the three products. As can be seen, the size-dependent metal-to-aerosol mass ratio generally exhibited a U-shaped distribution across the nanometer to micrometer size range. For active exposure, IQOS demonstrated a relatively lower metal-to-aerosol mass ratio in the smaller particle size range (nanometer to submicron) compared to the disposable e-cigarette and JUUL under both exposure conditions. Fig. 8 shows the size-dependent mass proportion (%) among the seven detected metals. Cr, Cu, Al, and Zn were the most abundant metals among the seven detected metals, whereas Ti, Pb, and V were found in relatively lower amounts. No clear patterns or correlations were observed between metal proportion and particle size.

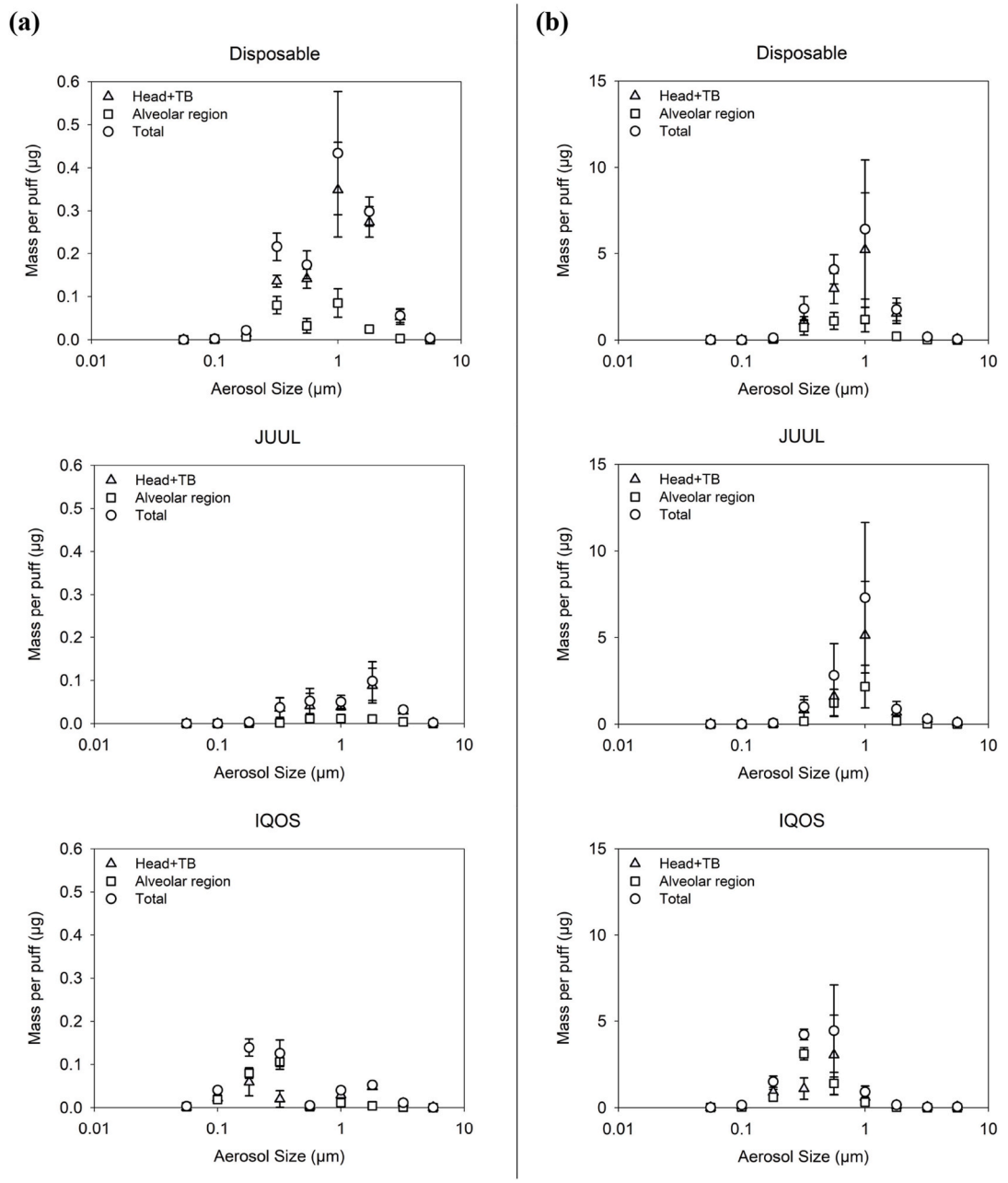


Fig. 6. Deposited mass of e-cigarette aerosol in human airways acquired by the MALDA-MOUDI approach for (a) active vaping and (b) passive vaping (N = 3).
(error bars indicating the standard deviation).

3.3. Health risk estimation

In this study, four of the seven metals identified in the ENDS and HTP aerosol—Cu, V, Pb, and Cr—are recognized for their potential to pose either non-cancer or cancer risks to humans. For instance, Cu exposure can cause respiratory irritation (CalEPA OEHHA: 0.1 mg/m^3), V can lead to lung damage (ATSDR MRLs: 0.0001 mg/m^3), and Pb is associated with neurological effects (EPA: B2; CalEPA OEHHA: CSF = 0.042 $(mg/kg\text{-}day)^{-1}$). Cr(VI) is the most toxic form of chromium and is classified as carcinogenic to humans (IARC Working Group on the Evaluation of Carcinogenic Risks to Humans, 2016). However, due to the limited published data on the proportion of Cr(VI) in the total Cr commonly detected in ENDS or HTP aerosol, the detected Cr in this study was conservatively assumed to be in the less toxic form, Cr(III), to prevent an unreasonable overestimation of the cancer risk associated with aerosol exposure. Excessive inhalation of Cr(III) can induce allergic sensitization and asthma (ATSDR MRLs: 0.0001 mg/m^3).

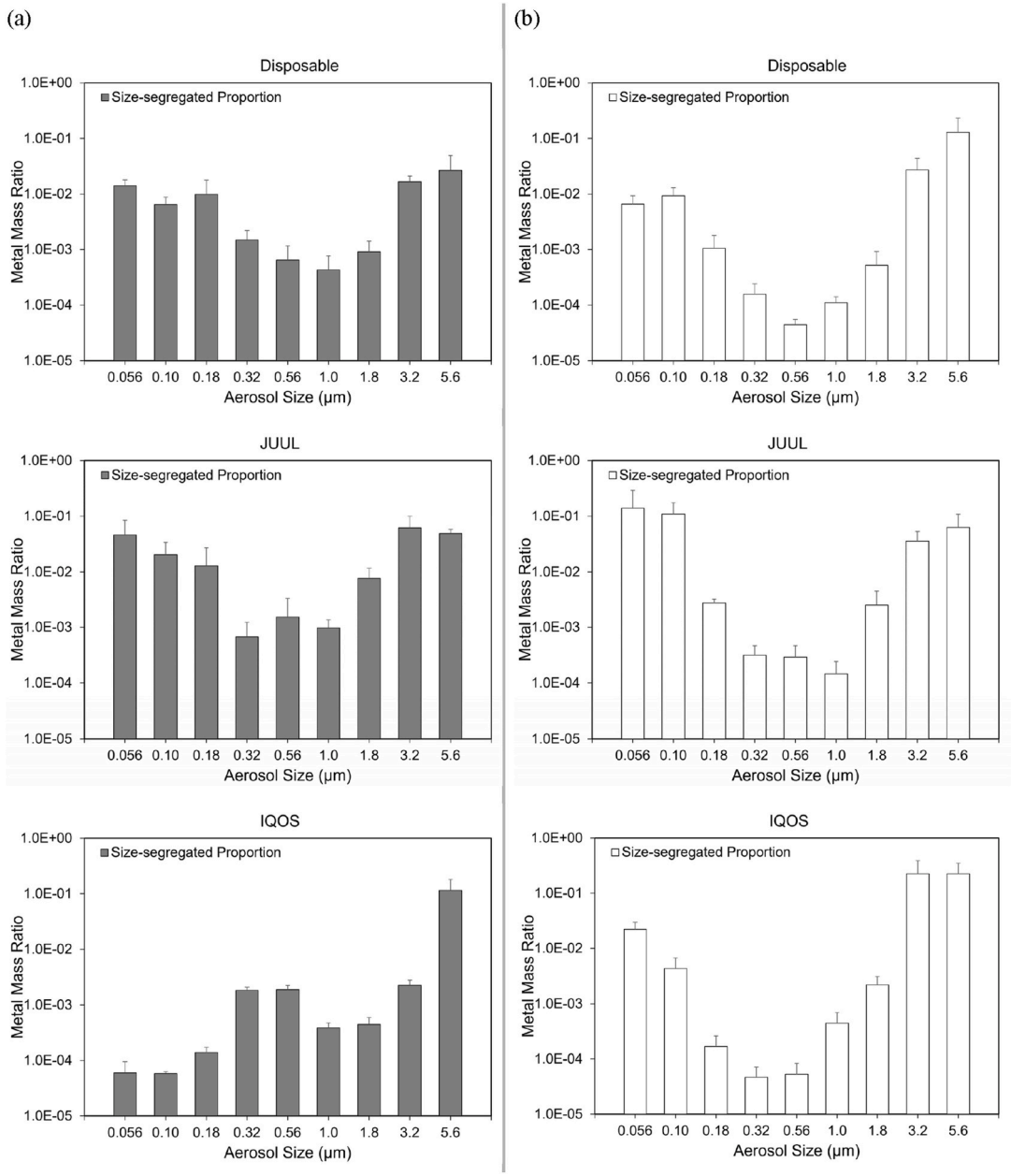


Fig. 7. Size-dependent metal mass ratio in aerosol for tested ENDS and HTP in conditions of (a) active exposure, and (b) passive exposure (N = 3). (error bars indicating the standard deviation).

Based on the acquired size-dependent respiratory deposited mass from MALDA-MOUDI experiments (Fig. 6), and the size-dependent metal constituent data from ICP-MS analyses (Figs. 7 and 8), health risks associated with the four toxic metals detected in the ENDS and HTP aerosol were estimated using Eqs. (7)–(12). Table 1 lists the calculated non-cancer and cancer risks for both active and passive exposure using the three products. For non-cancer risks, the values of *HQ* and *HI* were all below 1.0, indicating metal-induced non-cancer risks were within acceptable levels in both active and passive exposure. Vanadium (V) was identified as the primary contributor to non-cancer risk in this study. Among the tested products, IQOS showed a relatively higher non-cancer risk in active exposure ($HI = 0.329$), while the disposable e-cigarette posed the greatest risk in passive exposure ($HI = 0.650$). On the other hand, the cancer risks associated with active and passive exposure for the three products were also within acceptable limits, with excess lifetime cancer risk values ranging from 6.85×10^{-8} to 9.34×10^{-7}, all below the acceptable criteria of 1.0×10^{-6}.

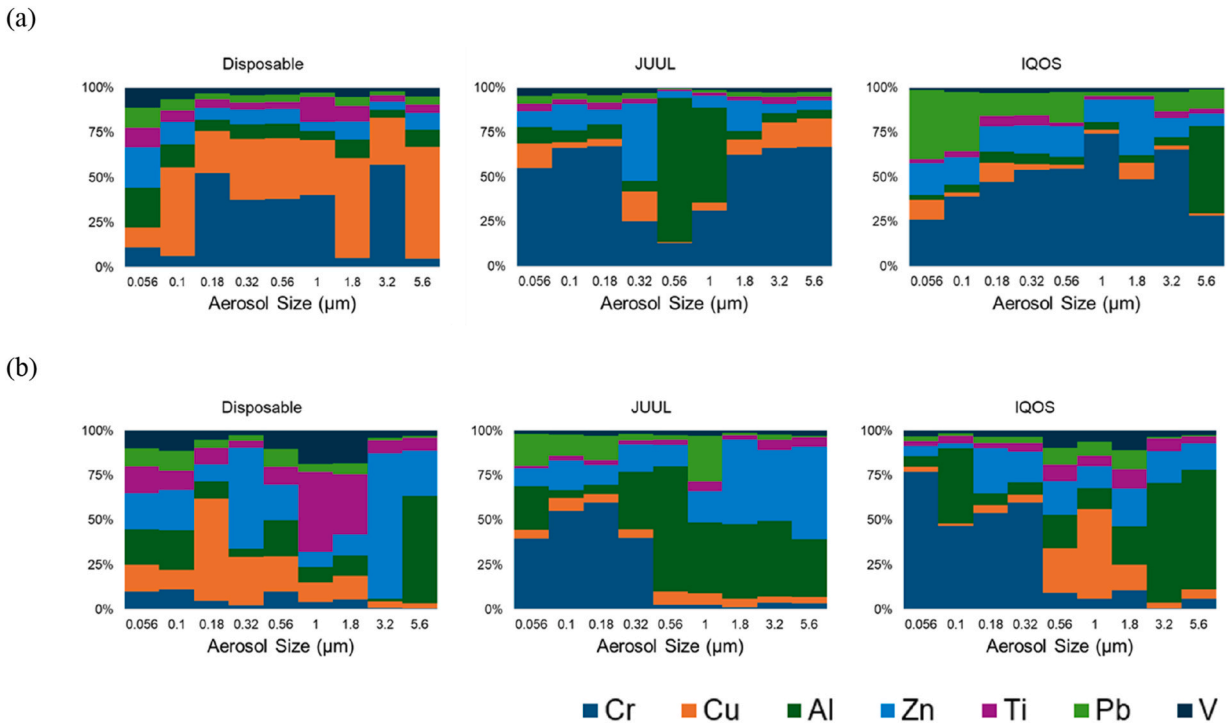


Fig. 8. Size-dependent proportion of seven detected metals in e-cigarette aerosol for different e-cigarettes in conditions of (a) active vaping and (b) passive vaping (N = 3).

4. Discussion

4.1. MALDA-MOUDI system

In aerosol respiratory deposition studies, the respiratory deposited mass is generally considered more informative than the respiratory deposition fraction for assessing health risks associated with aerosol exposure. In our previous studies, MALDA alone could only provide aerosol respiratory deposition fractions based on measurements of number-based particle size distributions. To further estimate the aerosol deposited mass in the airways, an assumption about the particle density of the aerosol of interest is required (Su et al., 2023). While this approach to estimating respiratory deposited mass is useful when a direct method for determining the actual density of the aerosol particle is unavailable, it introduces a degree of uncertainty in particle mass calculations. For instance, when estimating the mass of aerosol particles, particles are often approximated to be spherical to simplify the volume calculations. In addition, assumptions about particle density require presuming the chemical properties of the aerosol in question. These assumptions can introduce uncertainties and potential errors in the results, particularly for aerosol particles with inherently irregular shapes, such as soot, or those with complex chemical compositions, such as ENDS or HTP aerosol. The development of the MALDA-MOUDI approach effectively addresses these limitations of the number-based MALDA method. By eliminating the need for a particle sizer and the assumption of the particle density, the MALDA-MOUDI system serves as a useful experimental tool for systematically studying size-dependent respiratory deposited mass of particles (in this study, non-volatile particles generated from ENDS or HTP) in major human airway regions over a wide particle size range.

4.2. Aerosol respiratory deposition experiments

The e-cigarette aerosol generated by disposable e-cigarettes and JUUL revealed a bimodal pattern in the number-based particle size distribution. Similar bimodal distributions have been reported in several e-cigarette aerosol studies, with peaks typically showing in the 0.03–0.08 μm and 0.1–0.3 μm ranges (Delaval et al., 2019; Floyd et al., 2018; Mikheev et al., 2016; Papaefstathiou et al., 2020; Stefaniak et al., 2022). In contrast, the particle size distribution produced by IQOS exhibited a unimodal pattern, which is consistent with findings from other research on heated tobacco devices similar to IQOS (Delaval et al., 2019; Pacitto et al., 2018). The mass-based ENDS and HTP aerosol size distribution revealed a unimodal pattern in the mass-based particle size distribution (Fig. 3 (b)). Other studies that used cascade impactors have been reported with MMAD, in the 0.7–1.2 μm ranges (Kane & Li, 2021; Oldham et al., 2018; Oldham et al., 2023). The peak of the aerosol mass distribution existed between 0.56 and 1.0 μm in our study, but the MMADs from these studies were relatively higher than our results (~0.6 μm).

This study also observed that particle size distributions from passive exposure were slightly shifted toward larger sizes relative to

Table 1
Health risks caused by metals present in e-cigarette aerosol generated by (a) disposable e-cigarette, (b) JUUL, and (c) IQOS.

(a) Disposable							
			Cr(III)[a]	Cu	V	Pb	
Active	Non-Cancer	ADD[b]	0.065	0.071	0.007		
		HQ	0.042	0.002	0.216		HI: 0.260
	Cancer	LADD[b]				0.003	
		CR				1.35×10^{-7}	
Passive	Non-Cancer	ADD[b]	0.006	0.023	0.020		
		HQ	0.004	0.001	0.646		HI: 0.650
	Cancer	LADD[b]				0.004	
		CR				1.67×10^{-7}	
(b) JUUL							
			Cr(III)[a]	Cu	V	Pb	
Active	Non-Cancer	ADD[b]	0.157	0.028	0.007		
		HQ	0.102	0.001	0.218		HI: 0.321
	Cancer	LADD[b]				0.003	
		CR				1.36×10^{-7}	
Passive	Non-Cancer	ADD[b]	0.034	0.026	0.013		
		HQ	0.022	0.001	0.431		HI: 0.454
	Cancer	LADD[b]				0.012	
		CR				4.59×10^{-7}	
(c) IQOS							
			Cr(III)[a]	Cu	V	Pb	
Active	Non-Cancer	ADD[b]	0.162	0.015	0.007		
		HQ	0.105	<0.001	0.223		HI: 0.329
	Cancer	LADD[b]				0.024	
		CR				9.34×10^{-7}	
Passive	Non-Cancer	ADD[b]	0.032	0.013	0.007		
		HQ	0.021	<0.001	0.243		HI: 0.264
	Cancer	LADD[b]				0.002	
		CR				6.85×10^{-8}	

‡: The RfDs used in this study are 1.543 (μg/kg·day) for Cr(III), 30.86 (μg/kg·day) for Cu, and 0.031 (μg/kg·day) for V. The CSF of Pb used in this study is 3.89×10^{-5}(μg/kg·day)$^{-1}$.

[a] Every amount of the detected Cr was assumed to be insoluble Cr(III).

[b] The unit of ADD and LADD is μg/kg·day.

active use. This shift could be attributed to the hygroscopic growth of aerosol particles. As mentioned in the method section, the ENDS and HTP aerosol passed through a T and %RH conditioner before entering the MALDA-MOUDI system during passive exposure experiments. With the relative humidity inside the conditioner approaching 100 %, particle hygroscopic growth may occur (Asgharian et al., 2018; Pichelstorfer et al., 2016).

4.3. Metal analysis and health risk assessment

The findings of this study demonstrated that metal-induced non-cancer and cancer risks from both active and passive exposure were generally within acceptable levels. This outcome may be attributed to the low presence of metals in target ENDS or HTP aerosol. The blank-adjusted metal concentrations from ICP-MS analyses indicated that most target metals were below the instrument's detection limit (LOD) and marked as N.D.

One of the strengths of this study is its size-dependent approach for estimating metal-to-aerosol mass ratios in aerosol. Published studies have quantified metals in aerosol by analyzing bulk liquid (Gray et al., 2019; Hess et al., 2017; Olmedo et al., 2018) or total suspended aerosol (Goniewicz et al., 2014; Lerner et al., 2015). However, these approaches overlook the variations of metal concentrations in ENDS aerosol due to particle size changes. Aerosols generated from ENDS or HTP are expected to undergo evaporation in ambient air, which may lead to an increased proportion of non-evaporable metals in particles as particle size decreases. By measuring the size-dependent metal-to-aerosol mass ratio, the distribution of target metals across different aerosol sizes could be ideally revealed. Given that the aerosol respiratory deposition is also particle size-dependent, integrating these two size-dependent data sets allows for a more accurate estimation of the deposited mass of metals in the human airways, especially for passive exposure scenarios.

Chromium exists in the environment in three primary forms: elemental chromium (Cr), trivalent chromium (Cr(III)), and hexavalent chromium (Cr(VI)). Standard ICP-MS metal analyses do not identify the oxidation state of metals, including chromium (Beauval et al., 2016; Hess et al., 2017). In this study, all detected chromium was conservatively assumed to be Cr(III). Although the distribution of chromium oxidation states in e-liquids warrants further investigation, a prior study employing an integrated ICP-MS/ion-chromatography method reported no detectable Cr(VI) in any of the commercial e-liquids examined (Lavisetty et al., 2024). This approach is also consistent with several studies that made the same assumption and reported acceptable health risk levels

for chromium (Alcantara et al., 2023; K. Farsalinos et al., 2015). In contrast, other studies have assumed that all measured chromium is Cr(VI) for cancer risk assessment, leading to the calculated excess lifetime cancer risks ranging from 2.55×10^{-4} to 4.39×10^{-4}, far exceeding the conventionally acceptable level (Fowles et al., 2020; S. Zhao et al., 2023). Despite these differences, Farsalinos and Rodu (2018) have stated that the health risk of Cr(VI) from inhaling ENDS aerosol should be negligible. However, if Cr(VI) made up more than 0.07 % of the total chromium in this study, the cancer risks associated with active use of three products would surpass the acceptable level of 1.0×10^{-6}. For passive exposure, Cr(VI) would need to account for over 0.87 % of the total chromium for the associated cancer risk to be considered unacceptable. Studies have shown that Cr(III) can be oxidized to Cr(VI) when exposed to high temperatures ranging from 200 °C to 400 °C (Apte et al., 2006; Burton et al., 2019). Since heating coils of ENDS can reach temperatures between 100 °C and 350 °C (Chen et al., 2018; Li et al., 2021), the formation of Cr(VI) may occur under certain thermal atomization conditions. Given that the metal oxidation state is closely linked to device characteristics, such as atomizing power and heating coil material (Alcantara et al., 2023; Zhao et al., 2022), future studies could further explore how heating-related parameters influence the oxidation states of metals in ENDS aerosol.

It is worth noting that, in this study, the aerosol concentrations generated in passive exposure experiments were relatively higher than those typically found in real-world indoor environments such as rooms, homes, and stores (Geiss et al., 2015; Jeon et al., 2024; Lampos et al., 2019). This is because aerosol dilution was restricted within the stainless-steel chamber used, resulting in higher aerosol concentrations. Moreover, our approach to estimating passive exposure did not account for aerosol deposition in the active user's lungs. Previous studies on ENDS aerosols and their constituents exhaled by the users have reported that the major chemical constituents in directly inhaled aerosols were a few-to ten-fold higher than those found in exhaled aerosols (Oldham et al., 2021; Samburova et al., 2018; St Helen et al., 2016).

Although the aerosol concentration in the passive exposure experiments was artificially high, the estimated health risks associated with passive exposure remained at an acceptable level. The experimental conditions in this study can still represent some secondary ENDS or HTP aerosol exposure scenarios, particularly for passively exposed individuals in close proximity to active users. For passively exposed individuals in spaces that comply with building codes for ventilation or at greater distances from an active user, aerosol concentrations are expected to be significantly lower. Nevertheless, the laboratory passive exposure experiments presented in this study can serve as a worst-case scenario, offering a useful reference data set for future research on real-world passive exposure studies. Moreover, applying the MALDA-MOUDI tandem system in more realistic experimental settings, taking into account the period of ENDS and HTP use as well as their natural decay, as shown as several previous study (Maloney et al., 2016; Protano et al., 2017) can provide improved risk estimation, by considering both the level of exposure and respiratory deposition of ENDS and HTP aerosols and their chemical constituents.

Another limitation is that all deposition tests were conducted with a single, static adult airway replica; consequently, dynamic airway motion and inter-individual variation caused by age, disease status, or breathing pattern were not represented. In addition, although a fan was used to promote mixing during sampling, the aerosol may not have been completely homogeneous, and partial evaporation of semi-volatile constituents (e.g., glycerol, flavor aldehydes) due to the use of the fan could have biased the measured particle-size distribution. Finally, the study quantified only particulate metals; gaseous and non-metalic toxicants such as formaldehyde, acetaldehyde, and carbon monoxide were outside the analytical scope, so the overall health risk may have been underestimated.

5. Conclusion

In this study, a newly developed MALDA-MOUDI tandem system was effectively applied in a study to determine the deposited mass of ENDS and HTP aerosol in major airway regions for assessing metal-induced health risks associated with active and passive use. Through aerosol respiratory deposition experiments and metal analyses of ENDS and HTP aerosol, the MALDA-MOUDI approach provided robust data on size-dependent deposited mass of metals in major human airway regions. The results indicated that the estimated non-cancer and cancer risks associated with toxic metals in ENDS and HTP aerosol generally remained within acceptable levels for both active and passive exposure. The experimental approach used in this study presents a systematic method for evaluating potential health risks associated with aerosol exposure. The MALDA-MOUDI approach can be employed in future environmental and occupational aerosol exposure studies to comprehensively assess health risks posed by harmful aerosols.

CRediT authorship contribution statement

Jinho Lee: Writing – original draft, Validation, Investigation, Data curation. **Wei-Chung Su:** Writing – review & editing, Supervision, Methodology, Funding acquisition.

Declaration of competing interest

The authors declare that they have no known competing financial interests or personal relationships that could have appeared to influence the work reported in this paper.

Acknowledgment

This research was supported by a Pilot Award from the Gulf Coast Center for Precision Environmental Health, a National Institute of Environmental Health Sciences P30 Environmental Health Sciences Core Center (P30ES030285) at Baylor College of Medicine.

Additional support was provided by Grant R21ES031795 from the NIEHS, and by a Pilot Award from the Southwest Center for Occupational and Environmental Health, which is supported by the NIOSH T42 Educational Resource Center Training Grant (5T42OH008421) at the University of Texas Health Science Center at Houston.

Data availability

Data will be made available on request.

References

Agency for Toxic Substances and Disease Registry. ATSDR ToxGuides. https://wwwn.cdc.gov/TSP/ToxGuides/ToxGuidesLanding.aspx.

Aherrera, A., Aravindakshan, A., Jarmul, S., Olmedo, P., Chen, R., Cohen, J., Navas-Acien, A., & Rule, A. (2020). E-cigarette use behaviors and device characteristics of daily exclusive e-cigarette users in Maryland: Implications for product toxicity. *Tobacco Induced Diseases, 18*(November), 1–10. https://doi.org/10.18332/tid/128319

Alcantara, C., Chaparro, L., & Zagury, G. J. (2023). Occurrence of metals in e-cigarette liquids: Influence of coils on metal leaching and exposure assessment. *Heliyon, 9*(3), Article e14495. https://doi.org/10.1016/j.heliyon.2023.e14495

Ali, F. R. M., Diaz, M. C., Vallone, D., Tynan, M. A., Cordova, J., Seaman, E. L., Trivers, K. F., Schillo, B. A., Talley, B., & King, B. A. (2020). E-cigarette unit sales, by product and flavor type—united states, 2014–2020. *MMWR. Morbidity and Mortality Weekly Report, 69*(37), 1313–1318. https://doi.org/10.15585/mmwr.mm6937e2

Allen, J. G., Flanigan, S. S., LeBlanc, M., Vallarino, J., MacNaughton, P., Stewart, J. H., & Christiani, D. C. (2016). Flavoring chemicals in E-Cigarettes: Diacetyl, 2,3-Pentanedione, and acetoin in a sample of 51 products, including Fruit-, Candy-, and cocktail-flavored E-Cigarettes. *Environmental Health Perspectives, 124*(6), 733–739. https://doi.org/10.1289/ehp.1510185

American Society of Heating, Refrigerating and Air-Conditioning Engineers. (2023). *ASHRAE standard 55-2023*. Thermal Environmental Conditions for Human Occupancy.

Amorós-Pérez, A., Cano-Casanova, L., del Carmen Román-Martínez, M., & Lillo-Ródenas, M.Á. (2022). Solid matter and soluble compounds collected from cigarette smoke and heated tobacco product aerosol using a laboratory designed puffing setup. *Environmental Research, 206*, Article 112619.

Apte, A., Tare, V., & Bose, P. (2006). Extent of oxidation of Cr(III) to Cr(VI) under various conditions pertaining to natural environment. *Journal of Hazardous Materials, 128*(2–3), 164–174. https://doi.org/10.1016/j.jhazmat.2005.07.057

Areecheewakul, S., Adamcakova-Dodd, A., Givens, B. E., Steines, B. R., Wang, Y., Meyerholz, D. K., Parizek, N. J., Altmaier, R., Haque, E., O'Shaughnessy, P. T., Salem, A. K., & Thorne, P. S. (2020). Toxicity assessment of metal oxide nanomaterials using in vitro screening and murine acute inhalation studies. *NanoImpact, 18*, Article 100214. https://doi.org/10.1016/j.impact.2020.100214

Asgharian, B., Price, O. T., Rostami, A. A., & Pithawalla, Y. B. (2018). Deposition of inhaled electronic cigarette aerosol in the human oral cavity. *Journal of Aerosol Science, 116*, 34–47. https://doi.org/10.1016/j.jaerosci.2017.11.014

Beauval, N., Howsam, M., Antherieu, S., Allorge, D., Soyez, M., Garçon, G., Goossens, J. F., Lo-Guidice, J. M., & Garat, A. (2016). Trace elements in e-liquids—Development and validation of an ICP-MS method for the analysis of electronic cigarette refills. *Regulatory Toxicology and Pharmacology, 79*, 144–148. https://doi.org/10.1016/j.yrtph.2016.03.024

Bekki, K., Inaba, Y., Uchiyama, S., & Kunugita, N. (2017). Comparison of chemicals in mainstream smoke in heat-not-burn tobacco and combustion cigarettes. *Journal of UOEH, 39*(3), 201–207. https://doi.org/10.7888/juoeh.39.201

Bhatt, S. P., Kim, Y., Harrington, K. F., Hokanson, J. E., Lutz, S. M., Cho, M. H., DeMeo, D. L., Wells, J. M., Make, B. J., Rennard, S. I., Washko, G. R., Foreman, M. G., Tashkin, D. P., Wise, R. A., Dransfield, M. T., & Bailey, W. C. (2018). Smoking duration alone provides stronger risk estimates of chronic obstructive pulmonary disease than pack-years. *Thorax, 73*(5), 414–421. https://doi.org/10.1136/thoraxjnl-2017-210722

Bracken-Clarke, D., Kapoor, D., Baird, A. M., Buchanan, P. J., Gately, K., Cuffe, S., & Finn, S. P. (2021). Vaping and lung cancer – A review of current data and recommendations. *Lung Cancer, 153*, 11–20. https://doi.org/10.1016/j.lungcan.2020.12.030

Brown, J. S., Zeman, K. L., & Bennett, W. D. (2002). Ultrafine particle deposition and clearance in the healthy and obstructed lung. *American Journal of Respiratory and Critical Care Medicine, 166*(9), 1240–1247. https://doi.org/10.1164/rccm.200205-399OC

Burton, E. D., Choppala, G., Vithana, C. L., Karimian, N., Hockmann, K., & Johnston, S. G. (2019). Chromium(VI) formation via heating of Cr(III)-Fe(III)-(oxy) hydroxides: A pathway for fire-induced soil pollution. *Chemosphere, 222*, 440–444. https://doi.org/10.1016/j.chemosphere.2019.01.172

Buu, A., Hu, Y., Wong, S., & Lin, H. (2020). Comparing American college and noncollege young adults on e-cigarette use patterns including polysubstance use and reasons for using e-cigarettes. *Journal of American College Health, 68*(6), 610–616. https://doi.org/10.1080/07448481.2019.1583662

California Environmental Protection Agency. Air toxics hot spots program guidance manual for preparation of health risk assessments appendices A: Hot spots unit risk and cancer potency values. https://oehha.ca.gov/media/CPFs042909.pdf.

Chen, W., Wang, P., Ito, K., Fowles, J., Shusterman, D., Jaques, P. A., & Kumagai, K. (2018). Measurement of heating coil temperature for e-cigarettes with a "top-coil" clearomizer. *PLoS One, 13*(4), Article e0195925. https://doi.org/10.1371/journal.pone.0195925

Cheng, H. G., Noggle, B., Vansickel, A. R., Largo, E. G., & Magnani, P. (2025). Tobacco use, risk perceptions, and characteristics of adults who used a heated tobacco product (IQOS) in the United States: Cross-sectional survey study. *JMIR Formative Research, 9*, Article e57398. https://doi.org/10.2196/57398

Cheng, Y. S., Su, Y. F., Yeh, H. C., & Swift, D. L. (1993). Deposition of thoron progeny in human head airways. *Aerosol Science and Technology, 18*(4), 359–375. https://doi.org/10.1080/02786829308959610

Cohen, B. S., Sussman, R. G., & Lippmann, M. (1990). Ultrafine particle deposition in a human tracheobronchial cast. *Aerosol Science and Technology, 12*(4), 1082–1091. https://doi.org/10.1080/02786829008959418

Cullen, K. A., Ambrose, B. K., Gentzke, A. S., Apelberg, B. J., Jamal, A., & King, B. A. (2018). *Notes from the field:* Use of electronic cigarettes and any tobacco product among middle and high school students—United States, 2011–2018. *MMWR. Morbidity and Mortality Weekly Report, 67*(45), 1276–1277. https://doi.org/10.15585/mmwr.mm6745a5

David, G., Parmentier, E. A., Taurino, I., & Signorell, R. (2020). Tracing the composition of single E-Cigarette aerosol droplets in situ by laser-trapping and raman scattering. *Scientific Reports, 10*, 7929. https://doi.org/10.1038/s41598-020-64886-5

Delaval, M., Egli, D., Schüpfer, P., Benarafa, C., Geiser, M., & Burtscher, H. (2019). Novel instrument to generate representative e-cigarette vapors for physicochemical particle characterization and in-vitro toxicity. *Journal of Aerosol Science, 129*, 40–52. https://doi.org/10.1016/j.jaerosci.2018.11.011

Déry, R., Pelletier, J., Jacques, A., Clavet, M., & Houde, J. J. (1967). Humidity in anaesthesiology III. Heat and moisture patterns in the respiratory tract during anaesthesia with the semi-closed system. *Canadian Anaesthetists' Society Journal, 14*(4), 287–298. https://doi.org/10.1007/BF03003698

Farsalinos, K. E., & Rodu, B. (2018). Metal emissions from e-cigarettes: A risk assessment analysis of a recently-published study. *Inhalation Toxicology, 30*(7–8), 321–326. https://doi.org/10.1080/08958378.2018.1523262

Farsalinos, K., Voudris, V., & Poulas, K. (2015). Are metals emitted from electronic cigarettes a reason for health concern? A risk-assessment analysis of currently available literature. *International Journal of Environmental Research and Public Health, 12*(5), 5215–5232. https://doi.org/10.3390/ijerph120505215

Floyd, E. L., Queimado, L., Wang, J., Regens, J. L., & Johnson, D. L. (2018). Electronic cigarette power affects count concentration and particle size distribution of vaping aerosol. *PLoS One, 13*(12), Article e0210147. https://doi.org/10.1371/journal.pone.0210147

Fowles, J., Barreau, T., & Wu, N. (2020). Cancer and non-cancer risk concerns from metals in electronic cigarette liquids and aerosols. *International Journal of Environmental Research and Public Health, 17*(6), 2146. https://doi.org/10.3390/ijerph17062146

Geiss, O., Bianchi, I., Barahona, F., & Barrero-Moreno, J. (2015). Characterisation of mainstream and passive vapours emitted by selected electronic cigarettes. *International Journal of Hygiene and Environmental Health, 218*(1), 169–180. https://doi.org/10.1016/j.ijheh.2014.10.001

Goniewicz, M. L., Knysak, J., Gawron, M., Kosmider, L., Sobczak, A., Kurek, J., Prokopowicz, A., Jablonska-Czapla, M., Rosik-Dulewska, C., Havel, C., Jacob, P., & Benowitz, N. (2014). Levels of selected carcinogens and toxicants in vapour from electronic cigarettes. *Tobacco Control, 23*(2), 133–139. https://doi.org/10.1136/tobaccocontrol-2012-050859

Gray, N., Halstead, M., Gonzalez-Jimenez, N., Valentin-Blasini, L., Watson, C., & Pappas, R. S. (2019). Analysis of toxic metals in liquid from electronic cigarettes. *International Journal of Environmental Research and Public Health, 16*(22), 4450. https://doi.org/10.3390/ijerph16224450

Gray, N., Halstead, M., Valentin-Blasini, L., Watson, C., & Pappas, R. S. (2022). Toxic metals in liquid and aerosol from pod-type electronic cigarettes. *Journal of Analytical Toxicology, 46*(1), 69–75. https://doi.org/10.1093/jat/bkaa185

Hess, C. A., Olmedo, P., Navas-Acien, A., Goessler, W., Cohen, J. E., & Rule, A. M. (2017). E-cigarettes as a source of toxic and potentially carcinogenic metals. *Environmental Research, 152*, 221–225. https://doi.org/10.1016/j.envres.2016.09.026

Hinds, W. C., & Zhu, Y. (2022). *Aerosol technology: Properties, behavior, and measurement of airborne particles*. John Wiley & Sons.

Hubbs, A. F., Cumpston, A. M., Goldsmith, W. T., Battelli, L. A., Kashon, M. L., Jackson, M. C., … Sriram, K. (2012). Respiratory and olfactory cytotoxicity of inhaled 2, 3-pentanedione in sprague-dawley rats. *American Journal Of Pathology, 181*(3), 829–844. https://doi.org/10.1016/j.ajpath.2012.05.021

Hubbs, A. F., Goldsmith, W. T., Kashon, M. L., Frazer, D., Mercer, R. R., Battelli, L. A., … Castranova, V. (2008). Respiratory toxicologic pathology of inhaled diacetyl in sprague-dawley rats. *Toxicologic Pathology, 36*(2), 330–344. https://doi.org/10.1177/0192623307312694

IARC Working Group on the Evaluation of Carcinogenic Risks to Humans. (2016). Outdoor air pollution. In *IARC monographs on the evaluation of carcinogenic risks to humans* (Vol 109). IARC.

International Commission on Radiological Protection. (1994). Human respiratory tract model for radiological protection. *Annals of the ICRP, 24*(1–3). ICRP publication 66.

International Organization for Standardization. (2018). ISO 20768:2018 vapour products—Routine analytical vaping machine—Definitions and standard conditions. https://www.iso.org/standard/69019.html.

Jeon, J., He, X., Shinde, A., Meister, M., Barnett, L., Zhang, Q., Black, M., Shannahan, J., & Wright, C. (2024). The role of puff volume in vaping emissions, inhalation risks, and metabolic perturbations: A pilot study. *Scientific Reports, 14*(1), Article 18949. https://doi.org/10.1038/s41598-024-69985-1

Kane, D. B., & Li, W. (2021). Particle size measurement of electronic cigarette aerosol with a Cascade impactor. *Aerosol Science and Technology, 55*. https://doi.org/10.1080/02786826.2020.1849536, 505-214.

Kelly, J. T., Asgharian, B., Kimbell, J., & Wong, B. A. (2004). Particle deposition in human nasal airway replicas manufactured by different methods. Part I: Inertial regime particles. *Aerosol Science and Technology, 38*, 1036–1071. https://doi.org/10.1080/027868290883360

Lalo, H., Leclerc, L., Sorin, J., & Pourchez, J. (2020). Aerosol droplet-size distribution and airborne nicotine portioning in particle and gas phases emitted by electronic cigarettes. *Scientific Reports, 10*, Article 21707. https://doi.org/10.1038/s41598-020-78749-6

Lampos, S., Kostenidou, E., Farsalinos, K., Zagoriti, Z., Ntoukas, A., Dalamarinis, K., … Poulas, K. (2019). Real-time assessment of e-cigarettes and conventional cigarettes emissions: Aerosol size distributions, mass and number concentrations. *Toxics, 7*(3), 45. https://doi.org/10.3390/toxics7030045

Lavisetty, P., Collins, D., Pennington, A., Humphries, K., & Gillman, I. G. (2024). Speciation analysis of Cr(iii) and Cr(vi) in aged e-liquids containing benzoic acid using IC-ICP-MS. *77th tobacco science research conference, abstract 60/Poster*.

Lee, J., & Su, W. (2025). A new approach for simultaneous measurement of aerosol respiratory deposition and its chemical composition: Health risk assessment of metal engineered nanomaterials in consumer spray aerosols. *International Journal of Hygiene and Environmental Health, 267*, Article 114588. https://doi.org/10.1016/j.ijheh.2025.114588

Lerner, C. A., Sundar, I. K., Watson, R. M., Elder, A., Jones, R., Done, D., Kurtzman, R., Ossip, D. J., Robinson, R., McIntosh, S., & Rahman, I. (2015). Environmental health hazards of e-cigarettes and their components: Oxidants and copper in e-cigarette aerosols. *Environmental Pollution, 198*, 100–107. https://doi.org/10.1016/j.envpol.2014.12.033

Li, Y., Burns, A. E., Tran, L. N., Abellar, K. A., Poindexter, M., Li, X., Madl, A. K., Pinkerton, K. E., & Nguyen, T. B. (2021). Impact of e-Liquid composition, coil temperature, and puff topography on the aerosol chemistry of electronic cigarettes. *Chemical Research in Toxicology, 34*(6), 1640–1654. https://doi.org/10.1021/acs.chemrestox.1c00070

Logue, J. M., Sleiman, M., Montesinos, V. N., Russell, M. L., Litter, M. I., Benowitz, N. L., Gundel, L. A., & Destaillats, H. (2017). Emissions from electronic cigarettes: Assessing vapers' intake of toxic compounds, secondhand exposures, and the associated health impacts. *Environmental Science & Technology, 51*(16), 9271–9279.

Luo, Y., Wu, Y., Li, L., Guo, Y., Cetintas, E., Zhu, Y., & Ozcan, A. (2021). Dynamic imaging and characterization of volatile aerosols in E-Cigarette emissions using deep learning-based holographic microscopy. *ACS Sensors, 6*, 2403–2410. https://doi.org/10.1021/acssensors.1c00628

Maloney, J. C., Thompson, M. K., Oldham, M. J., Stiff, C. L., Lilly, P. D., Patskan, G. J., … Sarkar, M. A. (2016). Insights from two industrial hygiene pilot e-cigarette passive vaping studies. *Journal of Occupational and Environmental Hygiene, 13*(4), 275–283. https://doi.org/10.1080/15459624.2015.1116693

Man, S. F., Adams, G. K., & Proctor, D. F. (1979). Effects of temperature, relative humidity, and mode of breathing on canine airway secretions. *Journal of Applied Physiology, 46*(2), 205–210. https://doi.org/10.1152/jappl.1979.46.2.205

McAuley, T. R., Hopke, P. K., Zhao, J., & Babaian, S. (2012). Comparison of the effects of e-cigarette vapor and cigarette smoke on indoor air quality. *Inhalation Toxicology, 24*(12), 850–857. https://doi.org/10.3109/08958378.2012.724728

McKelvey, K., Popova, L., Kim, M., Chaffee, B. W., Vijayaraghavan, M., Ling, P., & Halpern-Felsher, B. (2018). Heated tobacco products likely appeal to adolescents and young adults. *Tobacco Control, 27*, s41–s47. https://doi.org/10.1136/tobaccocontrol-2018-054596

Mikheev, V. B., Brinkman, M. C., Granville, C. A., Gordon, S. M., & Clark, P. I. (2016). Real-time measurement of electronic cigarette aerosol size distribution and metals content analysis. *Nicotine & Tobacco Research, 18*(9), 1895–1902. https://doi.org/10.1093/ntr/ntw128

Miller, F. J., Asgharian, B., Schroeter, J. D., & Price, O. (2016). Improvements and additions to the multiple path particle dosimetry model. *Journal of Aerosol Science, 99*, 14–26. https://doi.org/10.1016/j.jaerosci.2016.01.018

Monsé, C., Raulf, M., Jettkant, B., van Kampen, V., Kendzia, B., Schürmeyer, L., … Bünger, J. (2021). Health effects after inhalation of micro-and nano-sized zinc oxide particles in human volunteers. *Archives of Toxicology, 95*, 53–65. https://doi.org/10.1007/s00204-020-02923-y

National Academies of Sciences, Engineering, and Medicine. (2018). *Public health consequences of e-cigarettes*. National Academies Press.

National Committee on Radiation Protection, Measurements. (1997). *Deposition, retention and dosimetry of inhaled radioactive substances*. NCRP Report. *125*.

Oberdörster, G., Oberdörster, E., & Oberdörster, J. (2005). Nanotoxicology: An emerging discipline evolving from studies of ultrafine particles. *Environmental Health Perspectives, 113*(7), 823–839. https://doi.org/10.1289/ehp.7339

Oldham, M. J., Jeong, L., Ozvald, A., & Gene Gillman, I. (2023). Comparison of the particle size distribution and vapor phase of electronic nicotine delivery systems using two impactors. *Contributions to Tobacco & Nicotine Research, 32*(4). https://doi.org/10.2478/cttr-2023-0012

Oldham, M. J., Sehgal, A., Cohen, G., Chen, J., Evans, B., & Heraldez, D. (2021). Room air constituent concentrations from use of electronic nicotine delivery systems and cigarettes using different ventilation conditions. *Scientific Reports, 11*(1), 1736. https://doi.org/10.1038/s41598-021-80963-9

Oldham, M. J., Zhang, J., Rusyniak, M. J., Kane, D. B., & Gardner, W. P. (2018). Particle size distribution of selected electronic nicotine delivery system products. *Food and Chemical Toxicology, 113*, 236–240. https://doi.org/10.1016/j.fct.2018.01.045

Olmedo, P., Goessler, W., Tanda, S., Grau-Perez, M., Jarmul, S., Aherrera, A., Chen, R., Hilpert, M., Cohen, J. E., Navas-Acien, A., & Rule, A. M. (2018). Metal concentrations in e-Cigarette liquid and aerosol samples: The contribution of metallic coils. *Environmental Health Perspectives, 126*(2), Article 027010. https://doi.org/10.1289/EHP2175

Pacitto, A., Stabile, L., Scungio, M., Rizza, V., & Buonanno, G. (2018). Characterization of airborne particles emitted by an electrically heated tobacco smoking system. *Environmental Pollution, 240*, 248–254. https://doi.org/10.1016/j.envpol.2018.04.137

Papaefstathiou, E., Bezantakos, S., Stylianou, M., Biskos, G., & Agapiou, A. (2020). Comparison of particle size distributions and volatile organic compounds exhaled by e-cigarette and cigarette users. *Journal of Aerosol Science, 141*, Article 105487. https://doi.org/10.1016/j.jaerosci.2019.105487

Pichelstorfer, L., Hofmann, W., Winkler-Heil, R., Yurteri, C. U., & McAughey, J. (2016). Simulation of aerosol dynamics and deposition of combustible and electronic cigarette aerosols in the human respiratory tract. *Journal of Aerosol Science, 99*, 125–132. https://doi.org/10.1016/j.jaerosci.2016.01.017

Protano, C., Manigrasso, M., Avino, P., & Vitali, M. (2017). Second-hand smoke generated by combustion and electronic smoking devices used in real scenarios: Ultrafine particle pollution and age-related dose assessment. *Environment International, 107*, 190–195.

Public Health England. (2016). *Use of e-cigarettes in public places and workplaces. Advice to inform evidence-based policy making.* Public Health England.

Samburova, V., Bhattarai, C., Strickland, M., Darrow, L., Angermann, J., Son, Y., & Khlystov, A. (2018). Aldehydes in exhaled breath during e-cigarette vaping: Pilot study results. *Toxics, 6*(3), 46. https://doi.org/10.3390/toxics6030046

Shehata, S. A., Toraih, E. A., Ismail, E. A., Hagras, A. M., Elmorsy, E., & Fawzy, M. S. (2023). Vaping, environmental toxicants exposure, and lung cancer risk. *Cancers, 15*(18), 4525. https://doi.org/10.3390/cancers15184525

Soneji, S., Barrington-Trimis, J. L., Wills, T. A., Leventhal, A. M., Unger, J. B., Gibson, L. A., Yang, J., Primack, B. A., Andrews, J. A., Miech, R. A., Spindle, T. R., Dick, D. M., Eissenberg, T., Hornik, R. C., Dang, R., & Sargent, J. D. (2017). Association between initial use of e-Cigarettes and subsequent cigarette smoking among adolescents and young adults: A systematic review and meta-analysis. *JAMA Pediatrics, 171*(8), 788. https://doi.org/10.1001/jamapediatrics.2017.1488

Staudt, M. R., Salit, J., Kaner, R. J., Hollmann, C., & Crystal, R. G. (2018). Altered lung biology of healthy never smokers following acute inhalation of E-cigarettes. *Respiratory Research, 19*(1), 78. https://doi.org/10.1186/s12931-018-0778-z

Stefaniak, A. B., Ranpara, A. C., Virji, M. A., & LeBouf, R. F. (2022). Influence of E-Liquid humectants, nicotine, and flavorings on aerosol particle size distribution and implications for modeling respiratory deposition. *Frontiers in Public Health, 10*, Article 782068. https://doi.org/10.3389/fpubh.2022.782068

St Helen, G., Havel, C., Dempsey, D. A., Jacob III, P., & Benowitz, N. L. (2016). Nicotine delivery, retention and pharmacokinetics from various electronic cigarettes. *Addiction, 111*(3), 535–544. https://doi.org/10.1111/add.13183

Su, W., Chen, Y., & Xi, J. (2019). A new approach to estimate ultrafine particle respiratory deposition. *Inhalation Toxicology, 31*(1), 35–43. https://doi.org/10.1080/08958378.2019.1576808

Su, W., Lee, J., Afshar, M., Zhang, K., & Han, I. (2024). Assessing community health risks from exposure to ultrafine particles containing transition metals in the greater Houston area. *Science of The Total Environment, 912*, Article 169067. https://doi.org/10.1016/j.scitotenv.2023.169067

Su, W., Lee, J., Zhang, K., Wong, S.-W., & Buu, A. (2023). Estimation of health risks caused by metals contained in E-Cigarette aerosol through passive vaping. *Toxics, 11*(8), 684. https://doi.org/10.3390/toxics11080684

Su, W., Wong, S., & Buu, A. (2021). Deposition of E-cigarette aerosol in human airways through passive vaping. *Indoor Air, 31*(2), 348–356. https://doi.org/10.1111/ina.12754

Tillery, A., Aherrera, A., Chen, R., Lin, J. J., Tehrani, M., Moustafa, D., … Rule, A. M. (2023). Characterization of e-cigarette users according to device type, use behaviors, and self-reported health outcomes: Findings from the EMIT study. *Tobacco Induced Diseases, 21*, 159. https://doi.org/10.18332/tid/174710

Uchiyama, S., Hayashida, H., Izu, R., Inaba, Y., Nakagome, H., & Kunugita, N. (2015). Determination of nicotine, tar, volatile organic compounds and carbonyls in mainstream cigarette smoke using a glass filter and a sorbent cartridge followed by the two-phase/one-pot elution method with carbon disulfide and methanol. *Journal of Chromatography A, 1426*, 48–55. https://doi.org/10.1016/j.chroma.2015.11.058

U.S. EPA. Integrated risk information system (IRIS). from https://www.epa.gov/iris. (Accessed 31 March 2024).

U.S. EPA. (1999). *Compendium of methods for the determination of inorganic compounds in ambient air*. EPA. https://www.epa.gov/sites/default/files/2019-11/documents/overvw3.pdf.

U.S. EPA. (2011). *Exposure factors handbook: 2011 edition.* National Center for Environmental Assessment.

Zhao, D., Ilievski, V., Slavkovich, V., Olmedo, P., Domingo-Relloso, A., Rule, A. M., Kleiman, N. J., Navas-Acien, A., & Hilpert, M. (2022). Effects of e-liquid flavor, nicotine content, and puff duration on metal emissions from electronic cigarettes. *Environmental Research, 204*, Article 112270. https://doi.org/10.1016/j.envres.2021.112270

Zhao, S., Zhang, X., Wang, J., Lin, J., Cao, D., & Zhu, M. (2023). Carcinogenic and non-carcinogenic health risk assessment of organic compounds and heavy metals in electronic cigarettes. *Scientific Reports, 13*(1), Article 16046. https://doi.org/10.1038/s41598-023-43112-y

Zhou, Y., & Cheng, Y.-S. (2005). Particle deposition in a cast of human tracheobronchial airways. *Aerosol Science and Technology, 39*(6), 492–500. https://doi.org/10.1080/027868291001385